Preliminary Evaluation of Passive Thermal Control for the Soil Moisture Active and Passive (SMAP) Radiometer

A. J. Mastropietro[1], Eug Kwack[2], Rebecca Mikhaylov[3], Michael Spencer[4], Pamela Hoffman[5], and Douglas Dawson[6]
Jet Propulsion Laboratory, California Institute of Technology, Pasadena, California, 91109

Jeff Piepmeier[7], Derek Hudson[8], and James Medeiros[9]
NASA Goddard Spaceflight Center, Greenbelt, Maryland, 20771

NASA's Earth observing Soil Moisture Active & Passive (SMAP) Mission is scheduled to launch in November 2014 into a 685 km near-polar, sun synchronous orbit. As one of the four first-tier missions recommended by the National Research Council's Committee on Earth Science and Applications from Space, SMAP will provide comprehensive global mapping measurements of soil moisture and freeze/thaw state in order to enhance understanding of the processes that link the water, energy, and carbon cycles. The primary objectives of SMAP are to improve worldwide weather and flood forecasting, enhance climate prediction, and refine drought and agriculture monitoring during its 3 year mission. The SMAP instrument architecture incorporates an L-band radar and an L-band radiometer which share a common feed horn and parabolic mesh reflector. The instrument rotates about the nadir axis at approximately 14 rpm, thereby providing a conically scanning wide swath antenna beam that is capable of achieving global coverage within 3 days. In order to make the necessary precise surface emission measurements from space, the electronics and hardware associated with the radiometer in particular must meet very tight short term (instantaneous and orbital) and long term (monthly and mission) thermal stabilities. Short term orbital stabilities, for example, must not exceed 0.6°C/orbit, while longer term mission drift must not exceed 15°C. Maintaining these tight thermal stabilities is quite challenging because the sensitive electronics are located on a fast spinning platform that can either be in full sunlight or eclipse, thus exposing them to a highly transient environment. In the interest of providing a low cost solution to proper thermal management of the instrument, a passive design approach was first implemented early in the design cycle. A Thermal Desktop model was created in order to help evaluate the passive design and assist the project with deciding if a more advanced active control scheme would be required in order to meet the tight stabilities with sufficient margin. This paper will discuss the preliminary thermal model predictions and summarize what thermal stabilities can be realistically achieved through passive means on a fast spinning platform exposed to both direct sunlight and eclipse in low Earth orbit.

The SMAP mission has not been formally approved by NASA. The decision to proceed with the mission will not occur until the completion of the National Environmental Policy Act (NEPA) process. Material in this document related to SMAP is for information purposes only.

[1] Thermal Engineer, Instrument Mechanical Thermal Subsystem, Mail Stop 125-123
[2] Lead Instrument Thermal Engineer, Instrument Mechanical Thermal Subsystem, Mail Stop 125-123
[3] Thermal Engineer, Instrument Mechanical Thermal Subsystem, Mail Stop 125-123
[4] Instrument Systems Engineer, Instrument Systems Engineering, Mail Stop 300-319
[5] Mechanical Thermal Subsystem PEM, Instrument Mechanical Thermal Subsystem, Mail Stop 303-422
[6] Radiometer System Engineer, Instrument Systems Engineering, Mail Stop 168-314
[7] Radiometer Scientist, Instrument Radiometer, Mail Stop 555.0
[8] Radiometric System Performance, Instrument Radiometer, Mail Stop 555.0
[9] Instrument Systems Engineer, Instrument Radiometer, Mail Stop 556.0

Nomenclature

α	=	Solar Absorptivity
AFT	=	Allowable Flight Temperature(s)
AK	=	Aluminized Kapton
β	=	Beta Angle
BOL	=	Beginning of Life
CBE	=	Current Best Estimate
CNS	=	Correlated Noise Source
dB	=	Decibel(s)
ε	=	Infrared Emissivity
ε^*	=	Effective Emissivity
EMC	=	Electromagnetic Compatibility
EOL	=	End of Life
EPS	=	Expanded Polystyrene
GSFC	=	Goddard Space Flight Center
HP	=	Horizontal Pole
IR	=	Infrared Energy
IFA	=	Integrated Feed Horn Assembly
JPL	=	Jet Propulsion Laboratory
K	=	Kelvin
MLI	=	Multi Layer Insulation
NASA	=	National Aeronautics and Space Administration
OMT	=	Orthomode Transducer
PDM	=	Product Delivery Manager
RBA	=	Reflector Boom Assembly
RBE	=	Radiometer Back End Electronics
RBEA	=	Radiometer Back End Assembly
RDE	=	Radiometer Digital Electronics
RF	=	Radio-Frequency
RFE	=	Radiometer Front End Electronics
RFEA	=	Radiometer Front End Assembly
rpm	=	revolutions per minute
S/C	=	Spacecraft
SIA	=	Spun Instrument Assembly
SMA	=	Spin Mechanism Assembly
SMAP	=	Soil Moisture Active and Passive
ST	=	Silvered Teflon
VP	=	Vertical Pole

I. Introduction

The Soil Moisture Active Passive (SMAP) Mission, targeted for launch by the National Aeronautics and Space Administration (NASA) in 2014, will make global measurements of soil moisture and its freeze/thaw state by implementing an active radar and a passive radiometer that share a common L-band feed horn and a conically scanning 6-meter mesh reflector antenna (see Figure 1). Direct observations of soil moisture and freeze/thaw state from space will allow significantly improved estimates of water, energy, and carbon transfers between the land and the atmosphere, which in turn will lead to enhanced weather and climate forecasts, and improved flood prediction and drought monitoring capability. Figure 2 summarizes the basic mission parameters.

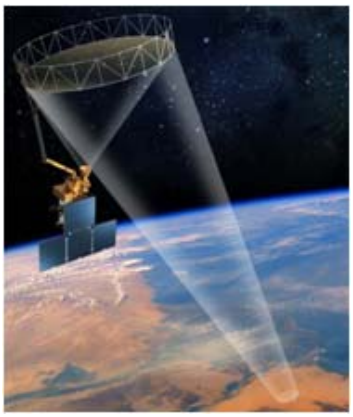

Figure 1. SMAP observatory with spinning 6m deployable mesh reflector antenna. The active radar and passive radiometer share a common L-band feed horn.

Orbit		Antenna	
Altitude	685 km	Main Reflector	6 meter mesh
Sun-synchronous	6 P.M. ascending	Spin Rate	14.6 rpms
Inclination	98°	Incidence Angle	40°
Coverage	2-3 day global	Swath	1000 km
L- Band Radiometer		L- Band Radar	
Frequency	1.41 GHz	Frequency	1.26 GHz
Relative Accuracy	1.5 K (soil moisture)	Relative Accuracy	0.5 dB (soil moisture) 0.7dB (freeze-thaw state)
Resolution	40 km (soil moisture)	Resolution	10 km (soil moisture) 3 km (freeze-thaw state)
Baseline 3 year mission life			

Figure 2. SMAP mission parameters.

Development of the SMAP instrument suite is by a partnership within NASA consisting of the Jet Propulsion Laboratory in Pasadena, California and the Goddard Spaceflight Center in Greenbelt, Maryland. GSFC is responsible for the radiometer and ground science data processing system, whereas JPL is responsible for the radar, overall instrument integration, and test and pre-launch mission management. Previously published papers[1][2][3][4][5] have already discussed the SMAP mission formulation including the measurement approach, preliminary mission requirements, and data products, and have summarized the state-of-the-art associated with existing active/passive L-band microwave systems. As shown in Figure 3, SMAP's unique nadir spinning antenna platform generates a large swath that enables better than 3 day global coverage. The rotating dual frequency radiometer and radar share a common feed, although only the radiometer has components located on the spinning platform. Signals are shared with rest of the S/C bus via slip rings.

L-band active/passive heritage applications include the Aquarius/SAC-D mission[6][7][8][9]. The Aquarius mission, due to launch in 2011, is flying both a scatterometer (radar) built by JPL and a radiometer built by GSFC that will measure sea surface salinity. While the two missions are often compared, there are some significant differences which are important to point out when discussing thermal designs: SMAP is a spinning instrument with a single feed horn exposed to the sun; Aquarius has 3 feed horns that are permanently shadowed by a sun shade on a non-spinning platform; Aquarius has a 2.5m fixed antenna versus SMAP's 6m boom deployable spinning antenna; and Aquarius has a much tighter thermal stability requirement of 0.1°C over 7 days versus 0.6°C per orbit for SMAP.

Currently the SMAP mission is nearing completion of phase B. Considerable mechanical and thermal design of the instrument has been accomplished. The objective of this paper is to present a description of the design process used for evaluating passive thermal control primarily for the SMAP radiometer. While the radar also requires careful thermal design, the radiometer in particular requires tight thermal stability control (0.6°C/orbit) in order to achieve the desired brightness temperature measurement accuracy of 1.5K.

II. Derivation of Thermal Stability Requirements

The overall science soil moisture error budget was flowed into a brightness temperature budget. Brightness temperature is a measure of the thermal radiated emissions from the soil, in this case measured by the radiometer at L-band. The instrument was given a portion of this brightness temperature error, which was further sub allocated to several major instrument error terms. One of these terms is the antenna temperature calibration, which is the term concerned with the error created in taking the digital numbers delivered by the instrument and translating them into brightness temperature at the input to the antenna. The major terms that make up the antenna temperature calibration are as follows:

1. Nonlinearity
2. **Feed to electronics input RF loss and emission**
3. Antenna mesh emissivity & temperature knowledge
4. Radiometer internal calibration sources temperature knowledge
5. Faraday Polarization rotation

The second component of this larger term drove the temperature stability goals. A simplified spreadsheet model of the RF losses and emission as a function of temperature was constructed. Given RF loss, temperature, and temperature stability inputs, this model would produce the corresponding brightness temperature error. An acceptable error based on the overall antenna temperature calibration error term was allocated for four time periods:

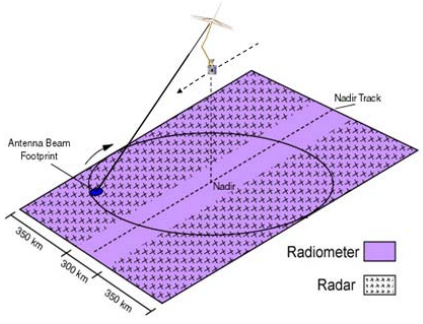

Figure 3. SMAP's spinning antenna generates a large swath for combined L-band radar and radiometer measurements.

instantaneous per minute rate, and change per orbit, month, and mission life. The spreadsheet allowed the thermal design team to quickly assess suitability of different temperatures and stabilities of the radiometer components.

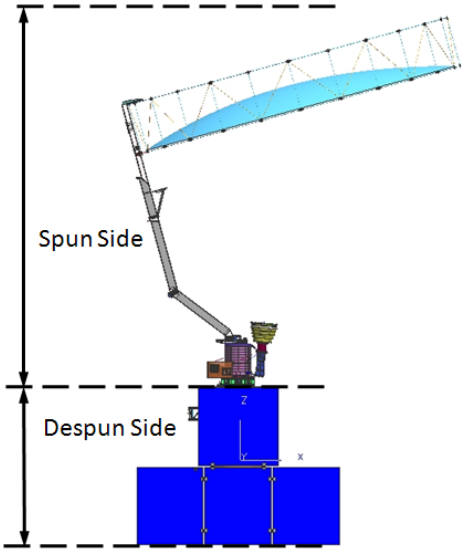

Figure 4. SMAP spacecraft with spinning instrument platform mounted on top of non-spinning bus.

The on-orbit thermal instabilities directly translate to noise in the system and must be minimized. Two passive thermal design configurations were considered and evaluated against the temperature and stability requirements.

III. Instrument Configuration

As shown in Figure 4, the SMAP observatory consists of the Spun Instrument Assembly (SIA) and the despun spacecraft bus. The despun bus serves as the mounting location for the fixed solar arrays and houses all of the avionics boxes and propulsion elements. Additionally, the bus provides the mounting location for the massive and thermally dissipative L-band radar components. The thermal design of the spinning radiometer segment of the observatory will be the focus of this paper.

The SIA consists of a cylindrical core structure that serves as both the housing for the Spin Mechanism Assembly (SMA) including slip rings and an RF rotary joint for passing the radar signal from the bus to the antenna, as well as the attachment foundation for 3 major subassemblies: the Reflector Boom Assembly (RBA), Integrated Feed Assembly (IFA), and the Radiometer Back End Assembly (RBEA).

The RBA, developed by Northrop Grumman Corporation, is a 6m lightweight mesh antenna that is mounted directly on top of the core structure. The RBA is stowed and locked alongside the spacecraft bus during launch, and then subsequently deployed for the science mission after arrival in orbit. The IFA and RBEA are the primary assemblies which make up the L-band radiometer. The IFA consists of a single feed horn connected to an Orthomode Transducer (OMT) via a thermal Isolator. The heart of the radiometer, known as the Radiometer Front End Assembly (RFEA), is mounted on the OMT. The RFEA contains the most thermally sensitive components of the radiometer. Within the RFEA, the following electronics are mounted upon a two tiered structural platform: 1 Radiometer Front End Electronics Box (RFE), 2 band pass filters, 2 Diplexers, 2 Couplers, and 1 Correlated Noise Source (CNS). The RFE is the component with the tightest thermal stability requirement. A cocoon of MLI is implemented around the RFEA to isolate the components from the environment.

The radar and radiometer share components and the RF dissipation generated during the radar transmit must be accounted for when developing the thermal design for the radiometer. The radar and radiometer signal chains are as follows:

- Radar: antenna→ feed horn→ OMT→ coupler→ diplexer→ rotary joint→ radar electronics located on bus
- Radiometer: antenna→ feed horn→ OMT→ coupler→ diplexer→ RFE→ RBE→ RDE

The RF dissipation from the radar is on the order of 10W and must also be accounted for in the RFEA and OMT.

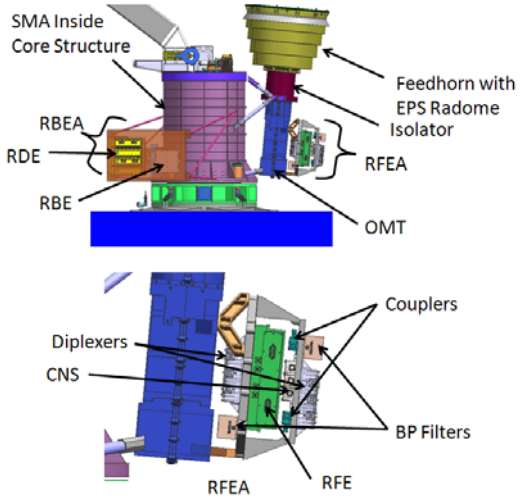

Figure 5. SMAP radiometer subassemblies with MLI cocoon removed.

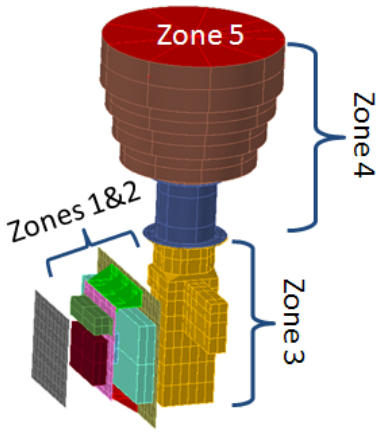

Figure 6. Thermal stability zones of the Radiometer IFA.

Radiometer Component	Zone	Short Term		Long Term	
		dT/dt (°C/min)	dT/orbit (°C/orbit)	Monthly (°C/month)	3 Year Mission Life (°C)
RFE	1	0.05	0.6	6.8	15
Diplexers, CNS, BP Filters, Couplers	2	N/A	1.2	6.9	15
OMT	3	N/A	2.4	7	19
Isolator & Feedhorn	4	N/A	8	8	30
Radome	5	N/A	120	60	100
RBE	N/A	0.1	N/A	N/A	N/A
RDE	N/A	0.5	N/A	N/A	N/A

Figure 7. SMAP instrument thermal stability requirements.

IV. Thermal Requirements

The allowable flight temperatures (AFTs) for operational radiometer components are -10°C to +30°C (-20°C to +55°C for non-operational conditions).

Thermal Stability Zones 1-5 were established to give the thermal engineer more flexibility with trading the configuration layout of the radiometer components (Figure 6). The first zone contains those components with the tightest thermal stability requirements and the fifth zone contains those with most relaxed requirements. The radiometer thermal stability requirements are derived from the radiometric accuracy budget and provided in Figure 7. Particularly challenging is the 0.6°C/orbit requirement for the RFE (Zone 1).

V. Thermal Environments

SMAP will be launched into a sun-synchronous 6 P.M. ascending orbit at an altitude of 685 km. Table 1 summarizes the relevant beta angles for the mission. Figure 8 depicts both the beta angle and solar constant variation as a function of time of year. Figure 9 is a schematic of SMAP viewed from the sun for β=58.5°. The eclipse season occurs when the beta angles are less than 65°, which occurs approximately from May 11 to August 2 of each year. When designing for the worst case thermal stabilities, a very conservative approach was taken whereby the maximum solar constant was applied at the minimum beta angle (longest eclipse duration). As can be viewed from the graph in Figure 8, this worst case stacking never realistically happens, but is typical of thermal analysis design process at this early stage in the design cycle.

Thermal Orbital Parameters	
Altitude	685 km
Mission Beta Angles	58.5°≤β≤89°
Period	89.9 minutes
Eclipse Beta Angles	58.5°≤β≤65°
Eclipse Season	83 days from May 11 August 2
Maximum Eclipse Duration	18 minutes

Table 1. SMAP orbital parameters.

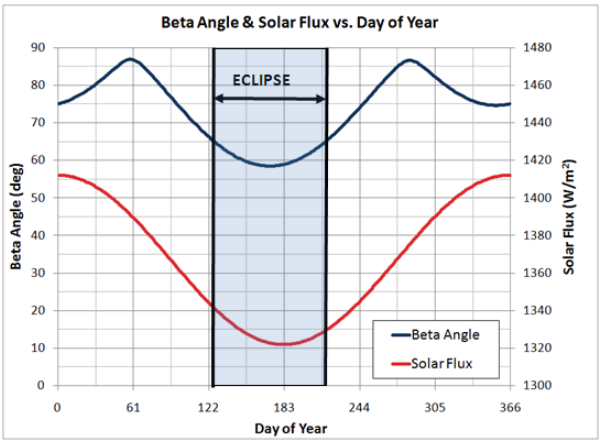

Figure 8. SMAP annual thermal environments.

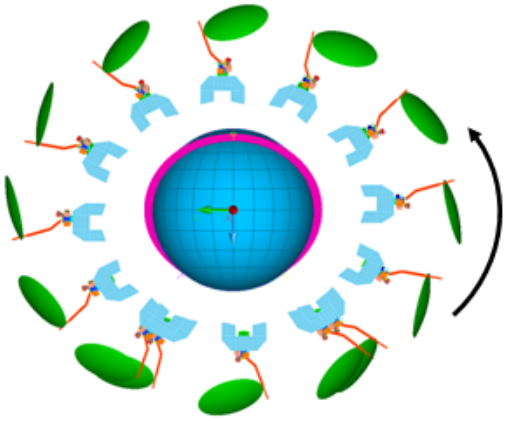

Figure 9. View from Sun (β=58.5°).

Environmental Parameter	Hot Case	Cold Case
Solar Constant	1420W/m²	1290W/m²
Earth IR	250W/m²	190W/m²*
Albedo Factor	0.35	0.25

Figure 10. SMAP Environmental Parameters.

The worst hot case occurs at higher beta angles when the sun is more fully incident on either the radiator or the feed horn. Figure 10 shows the environmental parameters assumed for worst hot and cold cases.

VI. Thermal Design Discussion

The RFE, diplexer 1, and band pass filter 1 are mounted on the RFE support plate which is supported from the OMT as shown Figure 11. Diplexer 2, both couplers, CNS and band pass filter 2 are mounted on the picnic table which is supported from the RFE support plate by two "L" shaped brackets. Inside the RFEA cocoon, components have low emittance surfaces to decouple the most sensitive components from the environment as much as possible.

The RBE and RDE design is relatively straightforward. Essentially the two electronic boxes are mounted on a radiator and enclosed within a cocoon. The RBEA enclosure assumes aluminized kapton MLI as the exterior blanket surface.

Early in the design process, the signal chain thermal dissipations were thought to be very small. As the design matured, dissipation increased and the RF dissipation due to the radar was determined to be much more of a contributing factor. With the smaller dissipation assumptions, design "A" seems more plausible. However, as time progressed, the second design "B" option proved to be more reliable and robust.

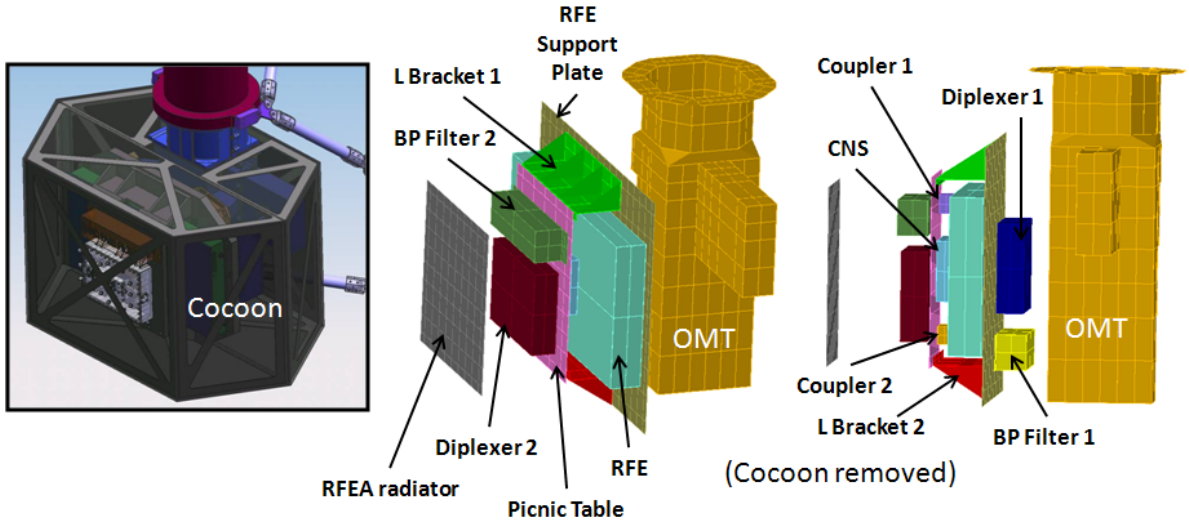

Figure 11. RFEA/cocoon configuration

A. Thermal "Design A" Description: Radiator on Feed Horn

The first design concept considered allows heat to radiate from the entire circumference of the feed horn. 10mil Silvered Teflon tape was assumed as the radiator thermal coating. The remaining parts of the feed horn assembly - Isolator, upper portion of the OMT, and the RFEA cocoon are covered with 5mil Silvered Teflon MLI blankets (teflon facing outside). A 3.34" thick EPS Radome covers the feed horn and acts as a fairly good insulator; making radiation out of the mouth of the feed horn was impractical. The Isolator is made out of aluminum in this design. The upper portion of the OMT requires thickened geometry in order to transport increased heat dissipation to the feed horn radiator.

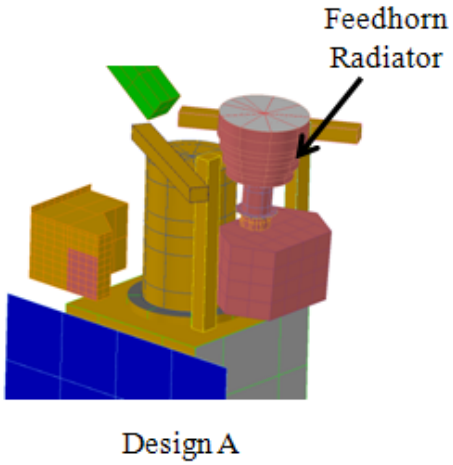

Figure 12. Radiometer Thermal Design A with Feed Horn Radiator.

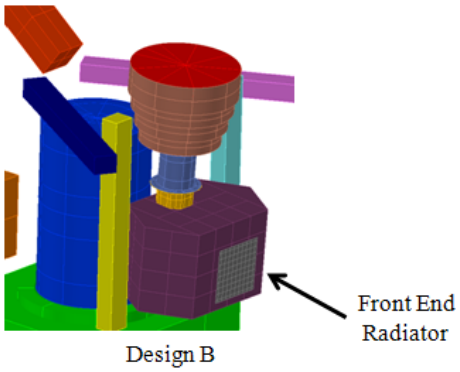

Figure 13. Radiometer Thermal Design B with Front End Radiator attached to RFEA.

B. Thermal "Design B" Description: Radiator attached to Front End Assembly

In this design approach, a dedicated front end radiator is attached to the RFEA picnic table. The radiator protrudes through the front end cocoon with an unobstructed view to space. The feed horn is blanketed with MLI and no longer serves as a radiator. The RFEA is not as thermally coupled to the OMT as in Design A since the primary heat transfer path is now from the picnic table structure to the new front end radiator. The Isolator is fabricated of Titanium and the OMT upper geometry not thickened in order to minimize the heat transfer to the feed horn. Both 5mil Silvered Teflon (ST) and Aluminized Kapton (AK) were evaluated as exterior surfaces for the MLI.

VII. Thermal Model Description and Assumptions

Thermal Desktop was used to develop a SMAP Instrument thermal model including the IFA and RFEA components as shown in Figures 14 and 15. The SMAP Spacecraft team created a thermal model of the spacecraft using the same tool; the instrument and spacecraft thermal models were merged and used for this study. Figure 15 shows the thermal model block diagram for Design B of IFA/RFEA including mass, power and conductance values. The mass values shown in the diagram were estimated from the thermal model, which are smaller than the mass CBE values. Although the Isolator material is assumed to be different in each design case, the mass in the thermal model is the same by assuming increased thickness for Design A. The power values shown are CBE plus uncertainty.

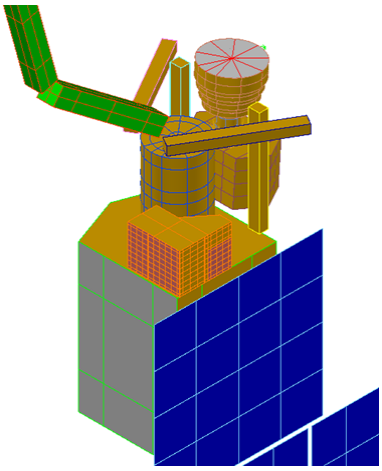

Figure 14. Thermal Desktop model of SMAP Instrument and S/C.

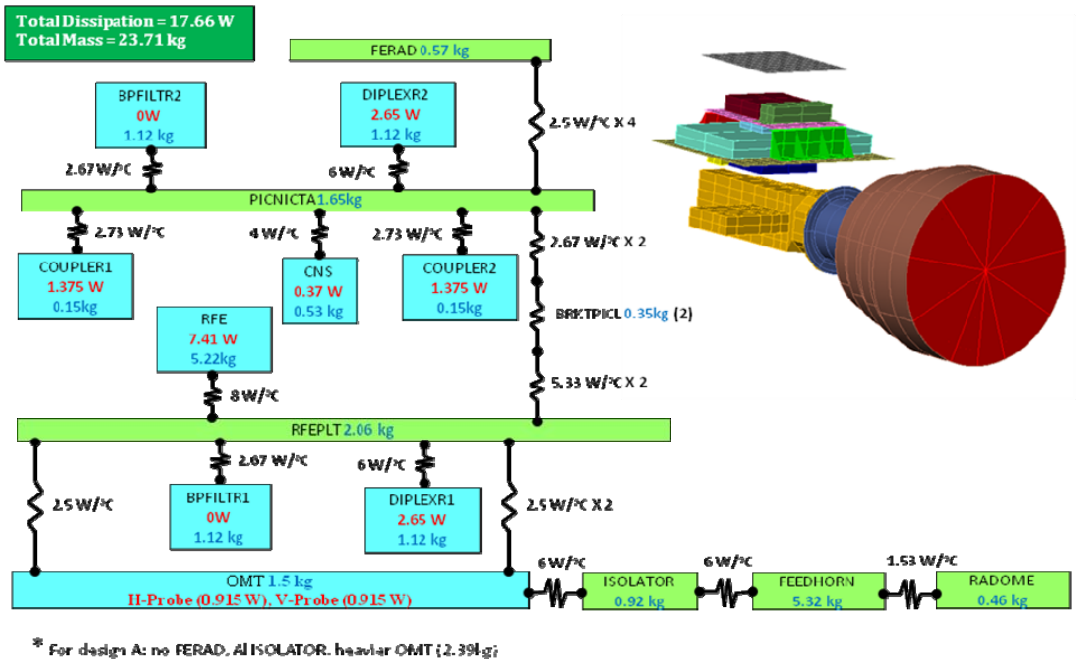

Figure 15. Thermal Model diagram of IFA/RFEA for Design B.

The supporting brackets from OMT to RFE support plate were not modeled and simple thermal resistances were used. The four brackets that support the RFEA radiator from the picnic table were still being designed and were also replaced by simple thermal resistances.

Thermo-optical properties are very important to the thermal analysis and EOL values of some materials are not readily available in open literature. The SMAP thermal team worked together with the GSFC Coatings Committee to determine the BOL and EOL material property values as shown in Figure 16 and Figure 17. Figure 18 summarizes the thermal analysis assumptions including power, mass, beta angle, environmental parameters, optical properties, MLI effective ε*, as well as S/C boundary conditions for the radiator sizing, orbital stability, monthly and mission life studies. The optical properties were linearly interpolated for monthly and mission studies. However, a value of 0.05 was added to solar absorptivity of Silvered Teflon during the first 6 months because of contamination.

Coating/Material	Solar Absorptivity, α	IR Emissivity, ε
	BOL/EOL	BOL/EOL
Silvered Teflon (10mil)	0.09/0.2	0.85/0.82
Silvered Teflon (5mil)	0.08/0.2	0.81/0.76
Interior MLI	N/A (never sees sun)	0.1/0.08
Bare Aluminum	N/A (never sees sun)	0.1/0.03
Bare Titanium	N/A (never sees sun)	0.18/0.08
Radome (ESP)	0. 20/0.33	0.90/0.7
Alodine (Chem Film)	N/A (never sees sun)	0.19/0.03
Clear Anodize (RBE/RDE)	N/A (never sees sun)	0.89/0.66

Figure 16. BOL and EOL optical properties

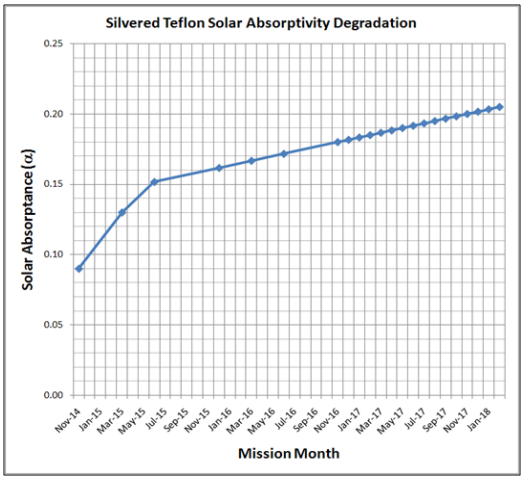

Figure 17. Assumed profile for Silvered Teflon solar absorptance degradation

Thermal Analysis Assumptions		
To Size Radiators: **Worst Case Hot for Science**	**To Assess Short Term Thermal Stabilities:** **Worst Stabilities for Science**	**To assess Mission Life and Monthly Stabilities:** **3 Year Mission Life and Month to Month Thermal Analysis**
• Highest Solar Flux • Highest Earth IR • Highest Albedo Factor • β=89° (No Eclipse) • Nominal ε* = 0.02 • CBE + Uncertainty for Dissipations • CBE Mass • EOL Optical Properties • S/C Despun Interface Modeled as +40°C Boundary	• Highest Solar Flux • Highest Earth IR • Highest Albedo Factor • β=58° (Maximum Eclipse Duration) • Nominal ε* = 0.02 • CBE + Uncertainty for Dissipations • CBE Mass • EOL Optical Properties • S/C Despun Interface modeled as +40°C Boundary	• Solar Flux interpolated from Fig. 8 • Earth IR Flux Interpolated (between 250 W/m² and 190 W/m²) Proportionally to Solar Flux Variation from Fig. 8 • Nominal Albedo • β interpolated from Fig. 8 • Nominal ε* = 0.02 • CBE + Uncertainty for Dissipations • CBE Mass • Optical properties linearly degraded over time to EOL values (includes initial 0.05 increase to ST α value due to contamination) • S/C Despun Interface Modeled as Time Varying Temperature Boundary

Figure 18. Thermal analysis assumptions for requirements verification.

VIII. Thermal Model Results and Discussion

Four thermal model cases were evaluated to address design trades and requirements. The steady state analysis determined the size of the radiators. The transient cases bounded the short term stability requirements. One year monthly run results evaluated nominal orbital and monthly stability requirements. Mission life requirements were addressed by completing results for an additional two years but only for March, June (valley) and November (peak) months.

A. Steady State Results

The worst hot case temperature conditions are during $\beta=89^o$ assuming hot environmental parameters. The hot $\beta=89^o$ case was used to size the radiators for Designs A and B. In Design A, the feed horn was initially covered with MLI and the side walls gradually opened to meet the RFE AFT limit of 30^oC. The final design left all side areas of the feed horn exposed and covered with $0.51m^2$ of 10mil Silvered Teflon tape. In Design B, the radiator was sized at $0.065m^2$. Design B evaluated two different cases with the use of Silvered Teflon tape (ST) or Aluminized Kapton (AK) for the exterior surface of the MLI. Handling, experience and cost concerns were the primary reasons for trading the exterior surface material for the MLI blankets; Aluminized Kapton MLI is preferable. The orbital averaged temperature map for hot $\beta=89^o$ is displayed in Figure 19.

For Design A, there is a gradual temperature gradient along the heat path. In this design, the Isolator no longer serves to restrict heat flow since it is fabricated from aluminum and has increased conductivity. The heat flows from the RFE (24.0°C), through the Isolator (4.5°C near OMT and -6.0°C near feed horn) and out from the feed horn (-21.3°C). In this case the hottest temperature occurs at Diplexer 2 (27.2 °C) which is mounted on the picnic table. For Design B ST, the main heat path is from the RFE to the RFEA radiator; only a small amount of heat (~1W) travels through the Isolator to the Radome since the Isolator in this design is made of Titanium. The RFE temperature is the

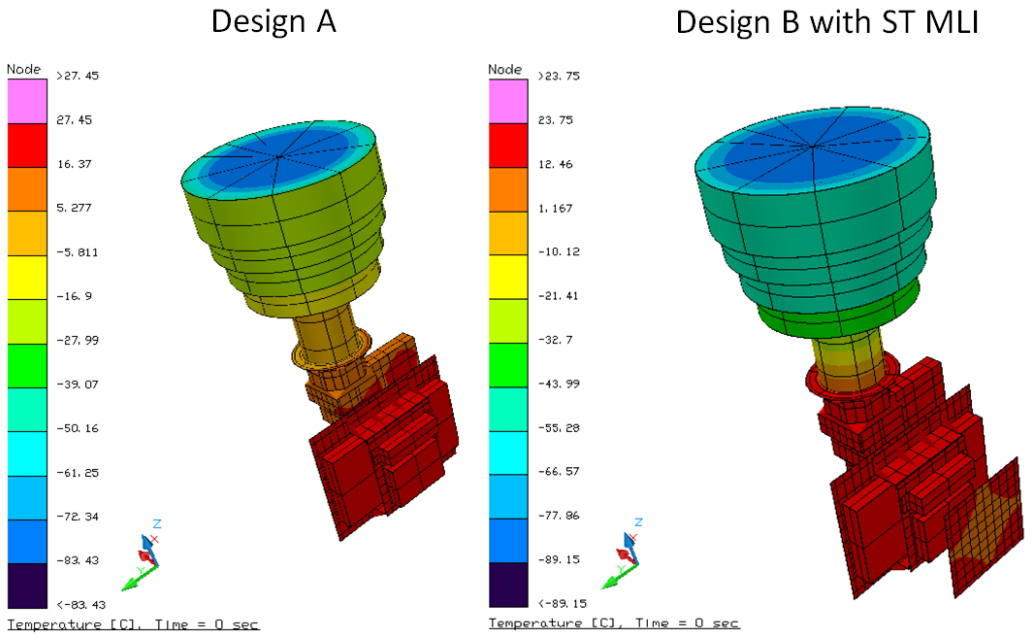

Figure 19. Orbital average temperature maps for Design A and Design B with ST MLI.

hottest at 23.5°C and temperatures gradually decrease for components mounted on the picnic table and at the RFEA radiator (11.8°C at the center). The temperature also decreases from the RFE along the OMT, Isolator and feed horn (-45.5 °C). Since the α/ε value of Silvered Teflon is small (0.23 at EOL), the feed horn temperature is very low even covered with ST MLI. The Isolator functions accordingly with a ΔT of 52.6°C (compared to 10.5°C for Design A).

The Radome is space facing through the porous reflector and does not receive direct sun for β=89°. Therefore, the outer layer temperatures are very cold (-92 °C for Design B ST). The Radome is bonded to the feed horn in both

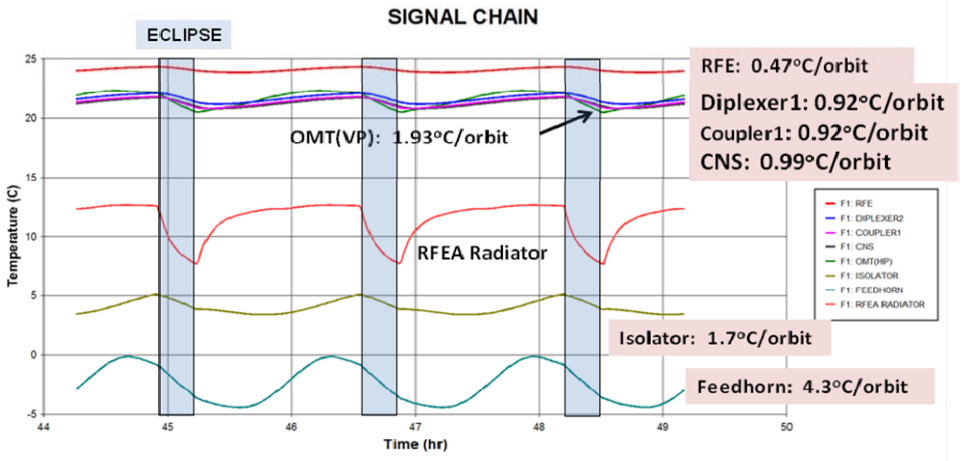

Figure 20. Transient temperature results for the RFEA and IFA for Design B with AK MLI.

designs, which results in a large radial temperature gradient (from 30°C to 86°C for Design A). Since the radome is quite thick, there is a large temperature gradient through the thickness: 58°C for Design A and 42°C for Design B ST.

For Design B with AK MLI, the RFEA temperatures rise by 2°C and the feed horn by more than 30°C due to the differing EOL α/ε values.

B. Orbital Transient Results

The worst case stability conditions occur during β=58° assuming hot environmental conditions. Design B with AK MLI is expected to have the worst case stability since the Silvered Teflon used in Designs A and B is intended to minimize solar effects. The transient results for the last 3 orbits out of 30 orbit results are shown in Figure 20. The orbital stabilities for the three cases are shown in Table 2.

Zone	Component	Design A	Design B ST	Design B AK	Requirement
1	RFE	0.14	0.32	0.47	0.7
2	Diplexer (Picnic Table)	0.16	0.78	0.99	1.2
3	OMT	0.57	1.22	1.93	2.4
4	Isolator	4.75	1.42	1.71	8
	Feedhorn (middle)	18.4	3.91	4.28	
5	Radome (outside center)	101	104	99	120

Table 2. Orbital stability results for the three design cases.

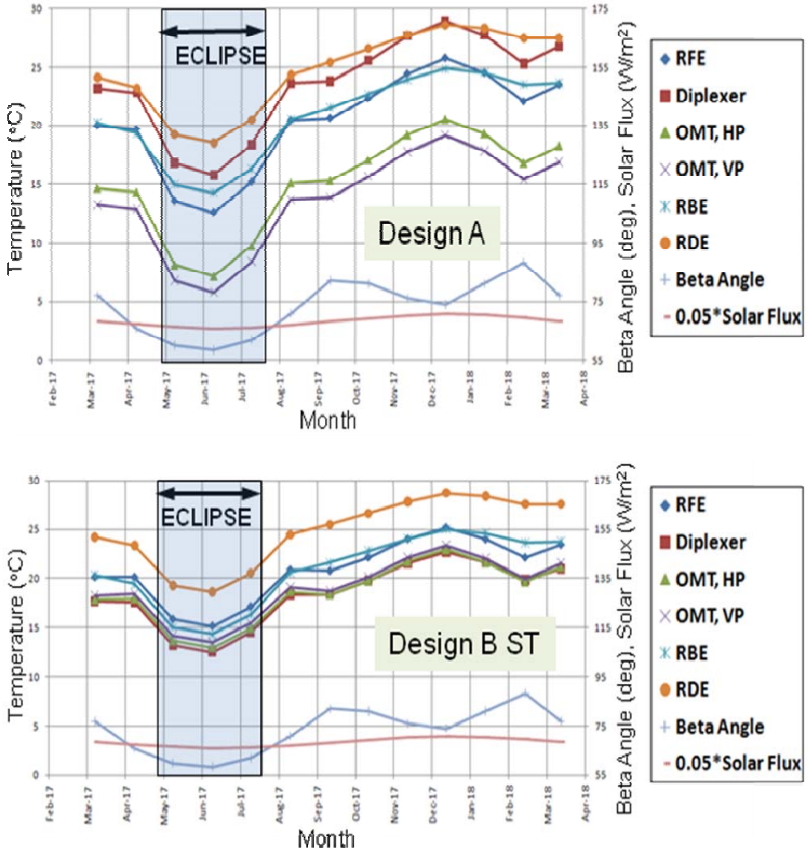

Figure 21. Monthly temperatures for Designs A and B ST

For Design A, Zones 1-3 show the best stability since these zones are far from the feed horn radiators. However, the feed horn stability at 18.4°C/orbit does not meet the 8°C/orbit requirement. RFEA components and the OMT are well protected from environmental changes by the MLI cocoon and Design B with either ST or AK MLI meets all orbital stability requirements. The RFE support plate components are more stable than the picnic table components since they are further from the RFEA radiator. The results for Design B with AK MLI are slightly larger than the ST results, yet still meet all requirements. The Radome stability requirements are applied at the middle of centerline. However, even results at the outside center in the table satisfy the requirement of 120°C/orbit. All three cases show large margin for the short term stability (less than 0.008°C/min against the 0.05°C/min requirement).

C. Monthly Results

The results of Design A and Design B with ST MLI are graphed for the last year of the mission (March 2017 to March 2018) with beta angle and solar flux plotted at the bottom of each figure (Figure 9 for temperatures and Figure 10 for orbital stabilities). In general, temperatures are lower during the eclipse season (May 11 to August 2)

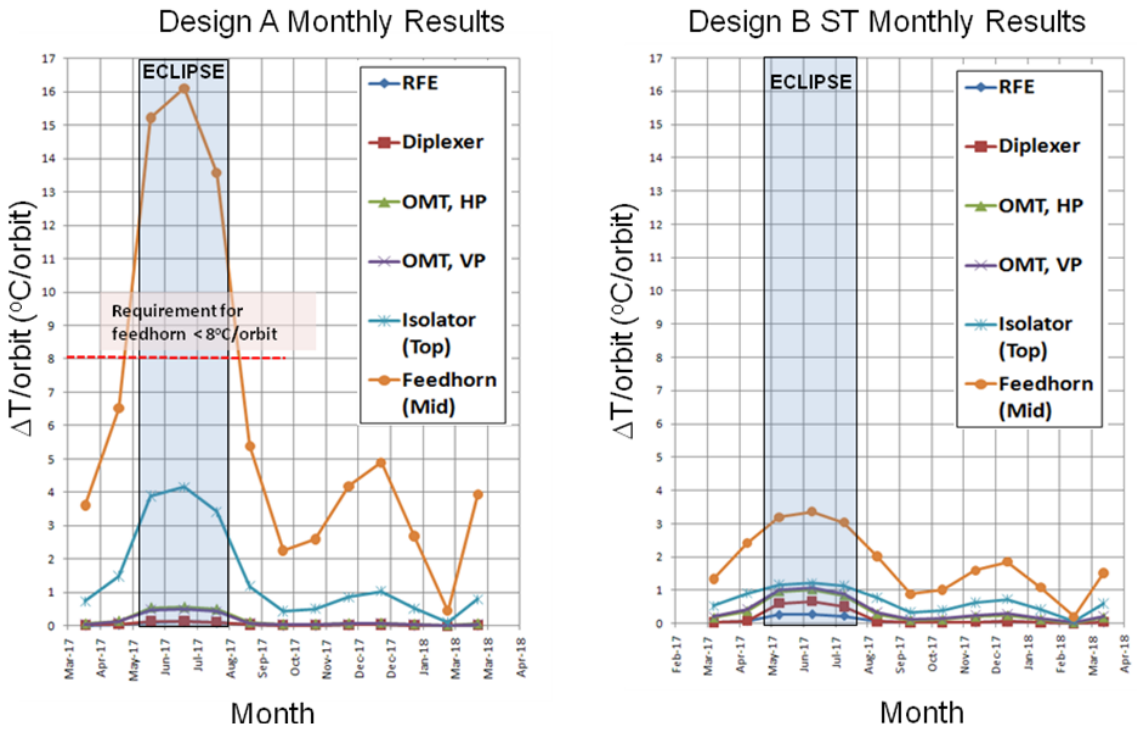

Figure 22. Monthly short term stability results for Designs A and B ST

but orbital variations are larger. The worst orbital stabilities occur at the middle of eclipse season, June 20th (β=59°). Design A shows the better stabilities for RFEA and OMT but variations of feed horn and Isolator for Design A are almost 4 times larger than those of Design B ST. Assuming nominal environmental parameters, the orbital variations are smaller than the worst case values shown in Figure 10. However, orbital stabilities for the feed horn still exceed the requirement during eclipse season. Due to optical property degradation, both designs increase in temperature by 3°C during the last year of the mission. For Design A, the temperature variation is less than 3°C/month except when the eclipse period begins and ends. In May, the changes are greater than 6°C/month; in August, less than 6°C/month. For Design B ST, the monthly temperature variation is not as extreme as Design A. Figures 21 and 22 illustrate the monthly temperature and stability results, respectively.

For better understanding of orbital stability changes during a year, the orbital variations are plotted as a function of the beta angle in Figure 23. It is interesting to note that the orbital variations are inversely proportional to the beta angle. For both designs, different slopes are observed, one for eclipse season and the other for non-eclipse season.

The detailed monthly stability behavior of the RFE is plotted in Figure 24 for three different

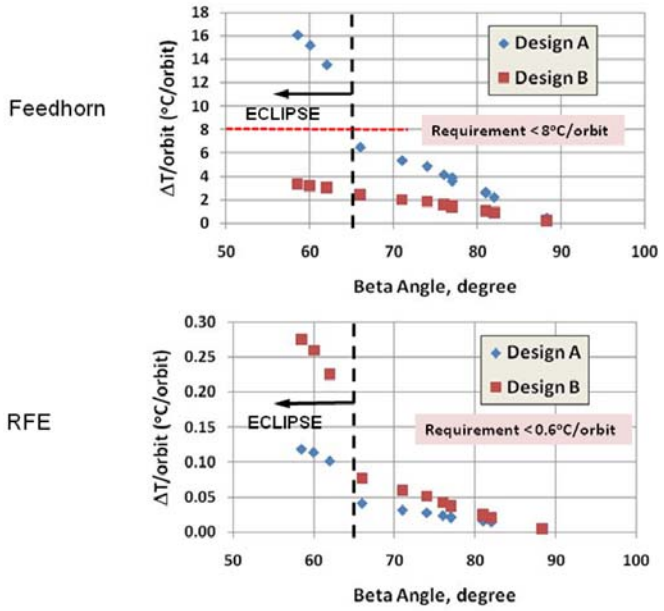

Figure 23. Orbital stability versus beta angle for Designs A and B

cases: Design A, Design B ST and Design B AK. Figure 25 shows similar results for the feed horn.

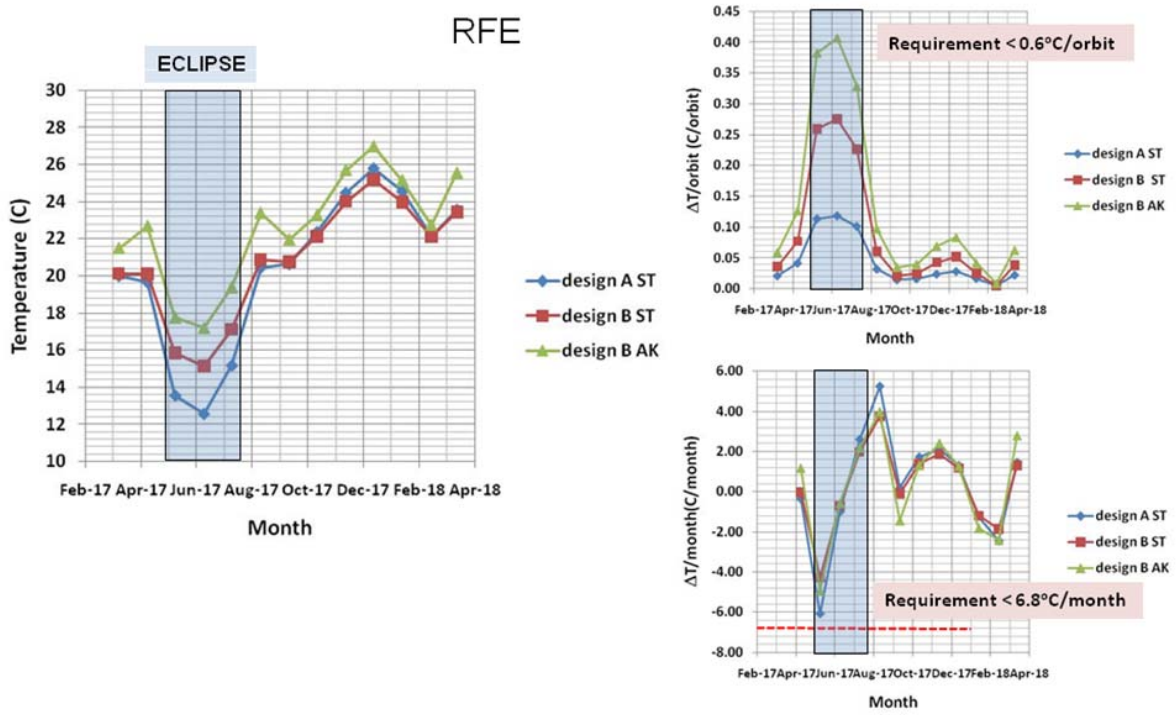

Figure 24. Monthly stabilities for the RFE for Designs A and B

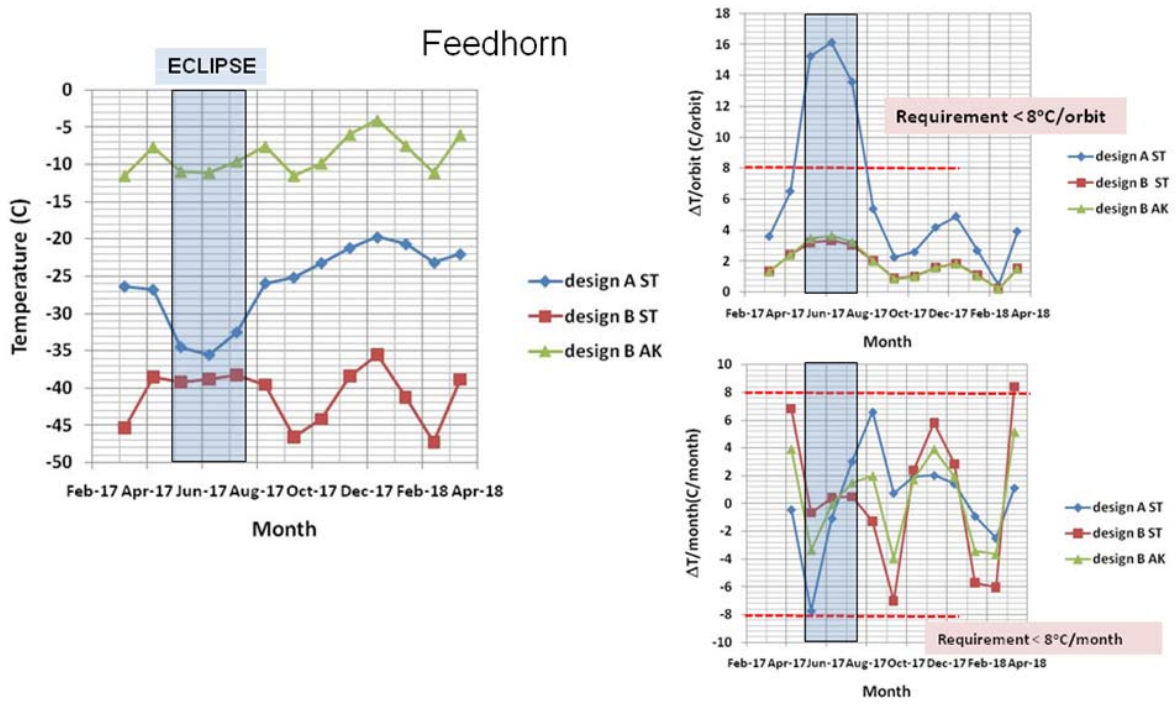

Figure 25. Monthly stabilities for the feed horn for Designs A and B

Design A – The RFE displays the same temperature behavior for both design cases. The feed horn temperature is different than Design B since the Isolator is aluminum and the feed horn is a fully exposed radiator. The orbital stability of the RFE and other RFEA components are more stable than Design B but the orbital variation of the feed horn does not meet the requirement. Although slightly larger than Design B, Design A meets all monthly stability requirements with a slim margin in the month that eclipse begins.

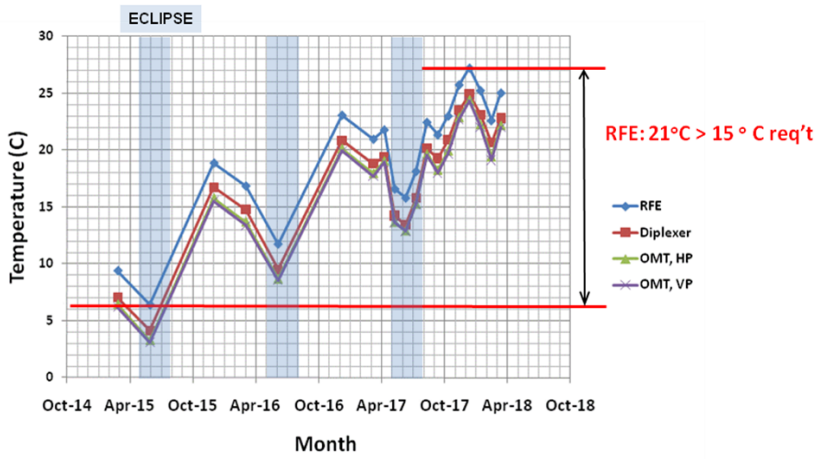

Figure 26. RFE mission life requirement

Design B – RFEA temperatures increase ~2°C from Design A. Design B AK feed horn temperature increased by 30°C over Design B ST due to EOL α/ε differences between ST (0.23) and AK (0.74). Design B meets all orbital and monthly stability requirements.

D. Mission Life Results

The RFE has a mission life requirement of temperature variation less than 15°C over 3 years. Figure 26 shows the peak to valley variation for the RFE over the 3-year mission life for Design B AK as 21°C. None of the three designs meet the mission life requirement (Design A variation is 25°C; Design B ST is 19°C). Table 3 is a compliance table of stability requirements for Design B AK.

A mitigation plan to achieve the 15°C mission life requirement was evaluated for each design case by addressing conservative assumptions: Silvered Teflon EOL value of 0.2 and Earth IR flux values of 190 and 250 W/m^2. Assuming a Silvered Teflon EOL of 0.18 instead of 0.2 would reduce the RFE temperature from 21°C to 17°C for Design B AK (19°C to 16°C for Design B ST). Using an IR flux range of 222 and 243 W/m^2 would decrease RFE temperatures by 3.5°C during eclipse season (June) and 0.5°C during peak (November) as shown in Figure 27.

Accounting for reduced EOL and Earth IR flux value range, the mission life stability would decrease from 21°C to 13°C for Design B AK, meeting the 15°C requirement. Design A would not meet the mission life stability at 18°C.

Radiometer Component	Zone	Short Term				Long Term			
		dT/dt (°C/min)		dT/orbit (°C/orbit)		Monthly (°C/month)		3 Year Mission Life (°C)	
		Req't	Predict	Req't	Predict	Req't	Predict*	Req't	Predict
RFE	1	0.05*	0.025*	0.6	0.47	6.8	5.3	15	21
Diplexers, Cal Noise Source, BP Filters, Couplers	2	N/A	N/A	1.2	0.99	6.9	5.3	15	21
OMT	3	N/A	N/A	2.4	1.93	7	5.4	19	21
Isolator & Feedhorn	4	N/A	N/A	8	4.3	8	5.1	30	21
Radome	5	N/A	N/A	120	38	60	11	100	21
RBE	N/A	0.1[b]	0.053	N/A	N/A	N/A	N/A	N/A	N/A
RDE	N/A	0.5[c]	0.08+	N/A	N/A	N/A	N/A	N/A	N/A
Radiometric Budgets (≤):		0.45 K				2.4 K		0.8 K	

* With IR = 190-250 W/m^2 as recommended by Aquarius Thermal Team
\+ Includes eclipse period, although not required

Table 3. Compliance table of stability requirements for Design B

IX. Conclusions

An Aquarius-like cocoon design was used to meet thermal stabilities passively for the SMAP radiometer. Design A covered all side walls ($0.51m^2$) of the feed horn with Silvered Teflon to act as a radiator. In Design B, a dedicated front end radiator ($0.065m^2$) was attached to the picnic table of the RFEA and protruded through the front end cocoon with an unobstructed view to space. Design A meets all short term and monthly stability requirements except for the feed horn orbital stability. Orbital stability is not met since the feed horn is exposed to the sun to serve as a radiator. Design B satisfies all the short term and monthly requirements utilizing Silvered Teflon or Aluminized Kapton for the exterior surface of the MLI. The mission life requirement of 15°C was not met for any design case: 25°C for Design A, 19°C for Design B ST, and 21°C for Design B AK. However, less conservative values utilized for Silvered Teflon EOL and the Earth IR flux range would allow Design B to meet mission life stability requirements. A passive design for the RFEA was developed to meet all temperature and stability requirements.

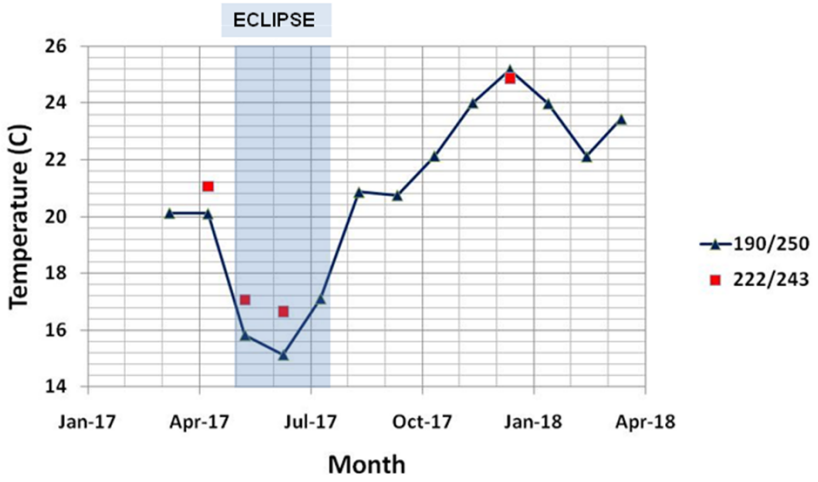

Figure 27. Effects of Earth IR flux values on RFE temperature for Design B ST

X. Acknowledgments

The development described in this paper was carried out at the Jet Propulsion Laboratory, California Institute of Technology, under a contract with the National Aeronautics and Space Administration. The authors express their thanks to the SMAP project sponsored by NASA for supporting this effort. The authors also wish to thank several of their colleagues at JPL who were instrumental to the radiometer passive thermal control study: Matthew Stegman and Frank Ramirez for their assistance with optimizing the mechanical layout and design of the IFA, Keith English and Tenny Lim for the mechanical accommodation of the Radiometer Back End Assembly, Paula Brown and Nelson Huang for their oversight of the RF and EMC performance of the shared radiometer components, Subha Comandur for supporting many iterations of the cabling layout for the ever evolving radiometer design, Morgan Hendry for making sure the SMAP instrument was spin balanced during each design iteration, Elizabeth Deems and Eric Slimko for requirements development and systems oversight, and Mark Duran for his expertise with thermal blankets and Silvered Teflon tape. The authors would also like to thank the following people who were involved with the numerous thermal reviews associated with the SMAP radiometer: Keith Novak, Eric Sunada, Gary Kinsella, Virgil Mireles, Art Avila, Ray Becker, Glenn Tsuyuki, Dan Nguyen, Jim Braley, and Walt Ancarrow. Lastly, the authors would also like to acknowledge Nick Emis, SMAP S/C Thermal Lead, for providing the instrument thermal team with the appropriate thermal model boundary conditions.

References

[1] Entekhabi, D., Njoku, E.G., O'Neill, P.E., Kellogg, K., Crow, W., Edelstein, W., et. al., "The Soil Moisture Active Passive (SMAP) Mission," *Proceedings of the IEEE,* Vol. 98, No. 5, IEEE, Boston, MA, 2010, pp. 704-716.

[2] Entekhabi, D., Njoku, E., O'Neill, P., Spencer, M., Jackson, T., Entin, J., Im, E., and Kellogg, K., "The Soil Moisture Active/Passive Mission (SMAP)," *Geoscience and Remote Sensing Symposium, 2008. IGARSS 2008. IEEE International,* Vol. 3, IEEE, 2008, pp. III - 1-III - 4.

[3] Entekhabi, D., Jackson, T.J., Njoku, E., O'Neill, P., Entin, J., "Soil Moisture Active/Passive (SMAP) Mission Concept," *Atmospheric and Environmental Remote Sensing Data Processing and Utilization IV: Readiness for GEOSS II,* SPIE, Vol. 7085, 2008, pp. 70850H-1-70850H-6.

[4] Kim, S., van Zyl, J., McDonald, K., and Njoku, E., "Monitoring surface soil moisture and freeze-thaw state with the high-resolution radar of the Soil Moisture Active/Passive (SMAP) mission," *Radar Conference, 2010 IEEE,* 2010, pp. 735-739.

[5] O'Neill, P., Entekhabi, D., Njoku, E., and Kellogg, K., "The NASA Soil Moisture Active Passive (SMAP) Mission: Overview," *Geoscience and Remote Sensing Symposium (IGARSS), 2010 IEEE International,* IEEE, 2010, pp. 3236-3239.

[6] Le Vine, D.M., Lagerloef, G.S.E., Colomb, F.R., Yueh, S., and Pellerano, F., "Aquarius: An Instrument to Monitor Sea Surface Salinity From Space," *Geoscience and Remote Sensing, IEEE Transactions on,* Vol. 45, No. 7, July 2007, pp. 2040-2050.

[7] Freedman, A., McWatters, D., and Spencer, M., "The Aquarius Scatterometer: An Active System for Measuring Surface Roughness for Sea-Surface Brightness Temperature Correction," *Geoscience and Remote Sensing Symposium, 2006. IGARSS 2006. IEEE International Conference on,* IEEE, 2006, pp. 1685-1688.

[8] McWatters, D., Freedman, A., Becker, R., Granger, J., Yates, P., Franklin, B., Borders, J., Yueh, S., Spencer, M., Price, D., Fischman, M., Cheetham, C., Paller, M., Pellerano, F., and Piepmeier, J., "Architecture and Design of the Aquarius Instrument for RF and Thermal Stability," *Radar Conference, 2009 IEEE,* IEEE, 2009, pp. 1-4.

[9] Yueh, S.H., Wilson, W.J., Edelstein, W., Farra, D., Johnson, M., Pellarano, F., Le Vine, D., and Hilderbrand, P., "Aquarius Instrument Design for Sea Surface Salinity Measurements," *Geoscience and Remote Sensing Symposium, 2003. IGARSS '03. Proceedings. 2003 IEEE International,* Vol. 4, 2003, pp. 2795-2797 v.